Journal of Catalysis 280 (2011) 104–115

Contents lists available at ScienceDirect

Journal of Catalysis

journal homepage: www.elsevier.com/locate/jcat

Multiple cycle reaction mechanism in the enantioselective hydrogenation of α,α,α-trifluoromethyl ketones

Z. Cakl [1], S. Reimann, E. Schmidt, A. Moreno, T. Mallat, A. Baiker *

Institute for Chemical and Bioengineering, Department of Chemistry and Applied Biosciences, ETH Zurich, Hönggerberg, HCI, CH-8093 Zurich, Switzerland

ARTICLE INFO

Article history:
Received 2 February 2011
Revised 8 March 2011
Accepted 9 March 2011
Available online 13 April 2011

Keywords:
Enantioselective
Diastereoselective
Hydrogenation
Platinum
Cinchona alkaloid
NMR
Trifluoromethyl ketone
Trifluoromethyl alcohol

ABSTRACT

The enantioselective hydrogenation of 2,2,2-trifluoroacetophenone (**1**) on cinchona-modified Pt, combined with the diastereoselective hydrogenation of cinchonidine and NMR analysis of the modifier–substrate–product interactions, revealed the key role of the product (*S*)-1-phenyl-2,2,2-trifluoroethanol (**2**) in enantioselection. We propose a multiple cycle mechanism including a racemic route (a) on the unmodified sites and three enantioselective routes. In the enantioselective cycles, there is an N–H–O type interaction between the quinuclidine N and the carbonyl O-atom of the substrate. At low conversion, the alkaloid alone is the source of chiral information (route *b*). With increasing conversion, the weakly acidic minor product (*S*)-**2** forms an adduct with the alkaloid and this complex controls the enantioselection (route *c*, lower ee). The frequently applied strong acid additive TFA replaces (*S*)-**2** and the alkaloid–TFA complex gives the highest ee (route *d*). The diastereoselective hydrogenation of cinchonidine disproves a former mechanistic model proposed in the literature.

1. Introduction

Early after discovering the enantioselective hydrogenation of α-ketoesters by Orito's group [1], it was generally considered that the Pt–cinchona system is highly specific to the transformation of the 1,2-dicarbonyl compounds α-ketoesters, α-ketoacids, and α-diketones [2,3]. The successful hydrogenation of 2,2,2-trifluoroacetophenone (**1**) to (*R*)-1-phenyl-2,2,2-trifluoroethanol (**2**, Scheme 1) with cinchonidine (CD)-modified Pt/alumina was the first evidence that the real structural requirement the substrate has to fulfill is the presence of an activating function in α–position to the carbonyl group [4]. In the past years, the research in the hydrogenation of α,α,α-trifluoroketones has revealed unique characteristics of this reaction class, compared with those of the mostly investigated transformation, the hydrogenation of α-ketoesters.

From a synthetic point of view, the most important deviation is the unusual substrate specificity of the Pt–cinchona system: Hydrogenation of **1** [5] and alkyl-4,4,4-trifluoroacetoacetates [6] afforded up to 96% ee, while the reaction is poorly selective with some aryl-substituted aromatic, benzylic, and particularly with aliphatic trifluoromethyl ketones [7–10].

From a mechanistic point of view, the differences fill a long list. In the hydrogenation of α-ketoesters, blocking the basic quinuclidine N atom of the alkaloid by alkylation or arylation eliminates the enantioselection, while *O*-methylation (to MeOCD) has only a minor effect on the ee [11,12]. This difference has been commonly interpreted as evidence for the involvement of the quinuclidine N in the activated complex leading to enantioselection and for the minor importance of the OH function [13–18]. *N*-methylation of CD leads to a loss of ee also in the hydrogenation of **1** and ethyl-4,4,4-trifluoroacetoacetate [19]. The influence of *O*-methylation is more complicated. In the hydrogenation of five different aryl-substituted 2,2,2-trifluoroacetophenones, the ee was almost completely lost or even the opposite enantiomer, the (*S*)-alcohol formed in small excess (4–11%), when CD was replaced with MeO-CD [5]. On the contrary, replacement of CD by MeOCD enhanced the ee from 70% to 90% in the hydrogenation of ethyl 4,4,4-trifluoroacetoacetate [20]. In some other cases, the effect of *O*-methylation depended also on the substituents in the substrate and on the solvent [8,19].

There are several more examples on the crucial role of the alcoholic OH function in enantioselection. In the hydrogenation of trifluoromethyl cyclohexyl ketone, replacement of toluene by EtOH inverted the ee with both CD and CN [21]. In two other instances, in the hydrogenation of adamantyl trifluoromethyl ketone and *tert*-butyl-trifluoromethyl ketone, the major product was inverted upon addition of 2-propanol [10]. Formation of the corresponding

* Corresponding author. Fax: +41 44 632 1163.
E-mail address: baiker@chem.ethz.ch (A. Baiker).
[1] Present address: On leave from Institute of Chemical Technology Prague, Department of Organic Technology, Technicka 5, 16628 Prague 6, Czech Republic.

0021-9517/$ - see front matter © 2011 Elsevier Inc. All rights reserved.
doi:10.1016/j.jcat.2011.03.009

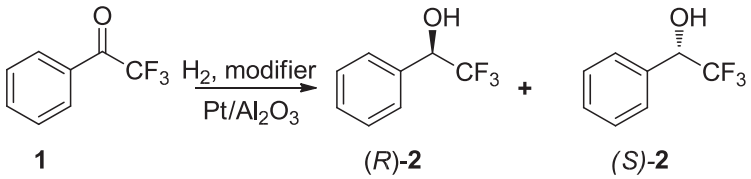

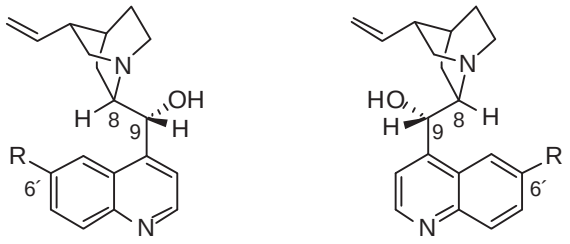

8 (*S*), 9 (*R*)		R	8 (*R*), 9 (*S*)		R
Cinchonidine	(CD)	H	Cinchonine	(CN)	H
Quinine	(QN)	OMe	Quinidine	(QD)	OMe

Scheme 1. Hydrogenation of 2,2,2-trifluoroacetophenone (**1**) on cinchona-modified Pt/Al_2O_3.

hemiketal with the solvent can diminish the ee at high conversion but cannot cause inversion of the major enantiomer [22]. NMR analysis also proved that no hemiketal was formed with the product α,α,α,-trifluoromethyl alcohol, as expected in the presence of the CF_3 group.

A thoroughly investigated phenomenon is the unpredictable effect of acid additives and solvents in this reaction class. In the hydrogenation of ethyl-4,4,4-trifluoroacetoacetate, replacement of the solvent toluene with AcOH doubled the ee and addition of TFA increased it further. In case of the 4′-CF_3 derivative of **1**, however, carboxylic acids diminished the ee. For comparison, in the hydrogenation of **1** and its aryl-substituted derivatives, replacement of CD with CD·HCl increased the ee under all conditions applied [5]. Obviously, the effect of carboxylic acids cannot simply be attributed to protonation of the quinuclidine N of CD, but rather H-bonding interactions have to be taken into account, as indicated by IR measurements [23,24].

Recently, Bartók's group reported numerous striking examples on the inversion of the major enantiomer by the addition of the strong acid TFA to the reaction mixture [10,25–28]. According to their interpretation of the unexpected inversion, a "nucleophilic intermediate complex" (N → C=O type interaction) between the alkaloid and ketone would be formed in the absence of TFA but even in the presence of AcOH. In contrast, in the presence of TFA, the protonated quinuclidine N of the alkaloid modifier would interact with the carbonyl O-atom of the substrate via an N–H–O type interaction. This assumption is rather astonishing, since an NMR study proved the complete protonation of the quinuclidine N of CD by 24 equivalents of AcOH [29]. The only additional effect of TFA was the protonation of the quinoline N, the transformation of which was negligible in AcOH. Bartók's concept focusing on the protonation of the quinuclidine N of the alkaloid by TFA also cannot rationalize the unexpected inversions in alcohols [10,21], whose solvents do not protonate CD.

Our opinion is fundamentally different. On the basis of DFT calculations [30,31] and in situ spectroscopic measurements [32,33], we assume an N–H–O type interaction between the quinuclidine N and the carbonyl O-atom even in a non-acidic medium. We attribute the frequently unpredictable behavior of the Pt–cinchona system in the hydrogenation of α,α,α-trifluoromethyl ketones to additional H-bonding interactions. This concept can rationalize the special effect of carboxylic acids [6,24]. Here, we present our novel observations on the role of the product in the hydrogenation of **1** and the evolution of competing enantioselective cycles during reaction.

2. Experimental section

2.1. Materials

2,2,2-Trifluoroacetophenone (**1**, 99%, Aldrich) was carefully distilled in vacuum before use. (±)-1-Phenyl-2,2,2-trifluoroethanol (**2**, >98%, Fluka), (*R*)-**2**, (⩾99.0%, Fluka), (*S*)-**2**, (⩾99.0%, Fluka), cinchonidine (CD, 98% NT, Fluka), cinchonine (CN, ⩾98% NT, Fluka), quinine (QN, 99%, Fluka), quinidine (QD, >99%, Acros), toluene (⩾99.7%, Fluka), trifluoroacetic acid (TFA, 99%, Acros), toluene D_8 (99.94%, Cambridge Isotop Lab., INC.), and chloroform D (99.8%, Armar Chemicals) were used as received. The 5 wt.% Pt/Al_2O_3 catalyst was purchased from Engelhard (Engelhard 4759).

2.2. Catalytic hydrogenations

The 5 wt.% Pt/Al_2O_3 catalyst was reduced at elevated temperature in a fixed-bed reactor prior to use. According to the standard procedure, the catalyst was heated under flowing nitrogen up to 400 °C in 30 min, followed by a reduction in flowing hydrogen for 60 min at the same temperature, and finally cooled down to

room temperature in flowing hydrogen in 30 min. At the end, the freshly reduced catalyst was purged with nitrogen for 10 min and then transferred immediately to the autoclave.

The enantioselective hydrogenations of **1** were carried out in a 25-ml stainless steel Parr autoclave equipped with a glass liner with PTFE cover and a magnetic stirrer, and a valve for sample collection or substrate injection. The pressure was controlled with a constant pressure regulator valve (Buchi BPC 9901). Under standard conditions 21 ± 1 mg of catalyst, 1.85 mmol of substrate and 3.4 μmol of modifier in 5 ml of toluene were stirred magnetically (1000 rpm) at 20 °C under a constant hydrogen pressure of 3 bars.

Hydrogenation of 2–4 mg (6.8–13.6 μmol) of CD was performed in a 50-ml stainless steel autoclave equipped with a glass liner with PTFE cover and a magnetic stirrer. The pressure was controlled with a constant pressure regulator valve (Buchi BPC 9901). Under standard conditions 42 ± 2 mg of catalyst, 10 ml of toluene were stirred magnetically (750 rpm) at 25 °C under a constant hydrogen pressure of 3 bars. Hydrogenation of CD was followed in the presence of **1** under the same conditions as described earlier for the hydrogenation of CD. 7.4 mmol of **1** was added either before starting the reaction or after a time delay of 30 min in the transient experiments. The standard procedure was applied also for the experiments in the presence of the hydrogenation products of **1**. Therein 3.7 mmol of either (*R*)-**2**, (*S*)-**2** or **2** has been added to the toluenic solution.

The conversion and enantioselectivity in the hydrogenation of **1** were determined by GC analysis, using an HP 6890 gas chromatograph equipped with a capillary column (CP-Chirasil-Dex CB, 25 m × 0.25 mm, i.d. 0.25 μm). Conditions: 80 °C for 2 min, 5 °C min^{-1} to 120 °C, 120 °C for 5 min, 8 °C min^{-1} to 180 °C, head pressure 1.5 bar He. Retention times (min): **1** 3.60, (*S*)-**2** 18.05, (*R*)-**2** 18.32. Products were identified by comparison with authentic samples and by GC–MS using an HP 6890 gas chromatograph equipped with an HP 5-MS column (25 m × 0.20 mm, i.d. 0.33 μm) coupled to an HP 5973 mass spectrometer.

The identification of the hydrogenated products of CD and the sample preparation is described elsewhere [34,35]. The estimated error in the determination of the enantiomeric excess (ee) and the diastereomeric excess (de) was about ±0.5% (at above 10% conversion) and that of the reaction rate (TOF) was in the range ±10%.

2.3. NMR measurements

Nuclear magnetic resonance (NMR) data were recorded on Bruker Avance 700 and DRX-400 spectrometers operating at the given spectrometer frequency. The samples were measured as solutions in $CDCl_3$ at ambient temperature and in non-spinning mode. The chemical shifts are expressed in parts per million (ppm) and referenced to tetramethylsilane (TMS) for the ^1H and ^{13}C spectra, and to $CFCl_3$ for the ^{19}F spectra [36]. Coupling constants *J* are given in Hz as absolute values.

2.3.1. PGSE measurements

All PGSE diffusion measurements were performed at a concentration of 2 mM using the standard stimulated echo pulse sequence [37] on a Bruker Avance DRX-400 spectrometer equipped with a microprocessor-controlled gradient unit and an inverse multinuclear probe with an actively shielded *Z*-gradient coil. The shape of the gradient pulse was rectangular, its duration δ was 1.75 ms, and its strength varied automatically in the course of the experiments. In the ^1H-PGSE experiments, Δ [38] was set to 117.75 ms and 167.75 ms, respectively, with a gradient recovery time of 100 μs. The number of scans per increment was 16 (in steps of 2–3% from 2–3% to 48–60%). A measurement of ^1H T_1 was carried out before each diffusion experiment and the recovery delay set to (at least) five times T_1. Typical experimental times were 2–4 h. For ^{19}F, Δ was set to 117.75 and 167.75 ms, respectively, with a gradient recovery time of 100 μs. Sixteen scans were taken with a recovery delay of 12–18 s (determined via a ^{19}F T_1 measurement), and a total experimental time of ca. 2.5–4 h.

All the spectra were acquired using 32 k points and processed with a line broadening of 1 Hz (^1H) and 2 Hz (^{19}F). The slopes of the lines, *m*, were obtained by plotting their decrease in signal intensity vs. G^2 using a standard linear regression algorithm. Normally, 12–20 points have been used for regression analysis and all of the data leading to the reported *D* values afforded lines whose correlation coefficients were >0.9995. We estimate the experimental error in *D* values at ±2%.

The diffusion coefficients reported were determined using the diffusion coefficient of HDO in D_2O as a reference ($D_{HDO} = 1.9 \times 10^{-9}\ m^2\ s^{-1}$), which afforded a slope of 1.976×10^{-4}. The data obtained were used to calculate the *D* values of the samples according to Eqs. (1) and (2) [38].

$$f = \left(\frac{\gamma_x}{\gamma_H}\right)^2 \left(\frac{\delta_x}{\delta_{HDO}}\right)^2 \frac{(\Delta - \delta/3)_x}{(\Delta - \delta/3)_{HDO}} \quad (1)$$

$$D_x = m_x * \frac{D_{HDO}}{m_{HDO}} * f \quad (2)$$

From the *D* values, the hydrodynamic radii of the ions were obtained via the Stokes–Einstein equation [39] and by introducing a semi-empirical estimation of the *c* factor [40,41]. The solvent viscosity ($10^{-3}\ kg\ s^{-1}\ m^{-1}$) used for the calculation of the hydrodynamic radii was η ($CHCl_3$) = 0.53.

2.3.2. 2D NOE measurements

^1H,^1H NOESY spectra were acquired on a Bruker Avance 700 spectrometer equipped with a multinuclear inverse probe. The concentration of the sample was 10 mM. For the NOESY experiment, the standard three-pulse (noesyph) [42] sequence was used with phase cycling by the TPPI method [43]. A relaxation delay of 800 ms was applied and the mixing time was 600 ms. The number of scans per increment was 32 (2 k data points), and 512 or 1 k experiments were acquired in the second dimension. Total experimental times were between 8–14 h. A QSINE weighting function was used in each dimension prior to Fourier transformation into a 2 k × 1 k data matrix.

The ^{19}F,^1H HOESY spectra were acquired using the standard four-pulse sequence (invhoesy) [44] on a Bruker Avance DRX-400 spectrometer equipped with a doubly tuned (^1H, ^{19}F) TXI probe. The concentration of the sample was 10 mM. A relaxation delay of 800 ms was applied and the mixing time was 800 ms. Typically, 16 transients were acquired into 2 k data points for each of the 512 or 1 k increments in t_1. Total experimental times were between 8 and 12 h. A QSINE(F1) and EM(F2) weighting function was used in each dimension prior to Fourier transformation into a 2 k × 1 k data matrix.

3. Results and discussion

3.1. Enantioselective hydrogenation of 2,2,2-trifluoroacetophenone (**1**): general aspects

We have mentioned in the introduction that in the hydrogenation of trifluoromethyl ketones, strong interactions with the solvent may blur the influence of other parameters. Because of the extended H-bonding among the reaction components, it is important to simplify the system with a weakly interacting solvent such as toluene. Attractive features of this solvent are the weak polarity, the weak H-bond donor and acceptor properties, and the reasonably good solubility of the cinchona alkaloids [45,46].

In preliminary experiments, we reinvestigated the role of some reaction parameters in toluene to provide a solid basis for the

present mechanistic study. Under standard conditions with 1.85 mmol of **1**, variation of the amount of modifier in the range 1.7 to 13.4 μmol gave an optimum of 44% ee to (*R*)-**2** with 3.4 μmol CD (0.68 mmol/l). The reaction rate slightly decreased with increasing amount of CD. These results are in line with earlier data obtained under different conditions for **1** [4] and trifluoromethyl cyclohexyl ketone [21].

A comparison of the enantioselective hydrogenations with the racemic reaction (Fig. 1) revealed higher rate ("ligand acceleration") [27,47–51] by addition of CD and CN, but a small rate deceleration in the presence of the 6′-methoxy derivatives QN and QD (Scheme 1). Under different conditions but also in toluene, Bartók and coworkers found rate acceleration with all four alkaloids in the same order as in Fig. 1 (CD > CN > QN > QD) [25]. Clearly, the presence of the 6′-methoxy function in QN and QD diminishes the reaction rate, and also the enantioselectivity as will be shown later.

Next, the effect of substrate concentration was investigated in the presence of CD. At conversions of 90–95% the ee increased from 30% to 52% by increasing the amount of **1** from 0.46 mmol to 5.5 mmol under otherwise standard conditions (not shown). In addition, increasing substrate concentration had a negative effect on the reaction rate, in agreement with former observations [4,21].

The behavior of all four modifiers is compared in Fig. 2 at two different concentrations. The reaction rate in the hydrogenations with CN, QN, and QD showed the same behavior as in the case of CD: higher substrate concentrations were detrimental to the rate. In the presence of CD and QN, a decrease in the substrate concentration by a factor of four diminished the ee by ca. 10–15%, but the major product remained (*R*)-**2**. In case of CN and QD, however, the lower substrate concentration resulted in the inversion of the major product from (*S*)-**2** to (*R*)-**2**. (Note that the differences with QD were small but well reproducible). This inversion has the astonishing consequence that at low substrate concentration, all cinchona alkaloids afford the same major product, (*R*)-**2**, independent of the configurations at C8 and C9 (Scheme 1).

Bartók and coworkers used low substrate concentration in toluene and also found (*R*)-**2** as the major product with all four alkaloids [25]. Interestingly, this is the starting point of their mechanistic model mentioned in the introduction [27], where they assume that protonation of the quinuclidine N of the alkaloids by TFA is necessary to arrive at the "usual" product distribution: (*R*)-**2** with CD and QN and (*S*)-**2** with CN and QD. However, the data

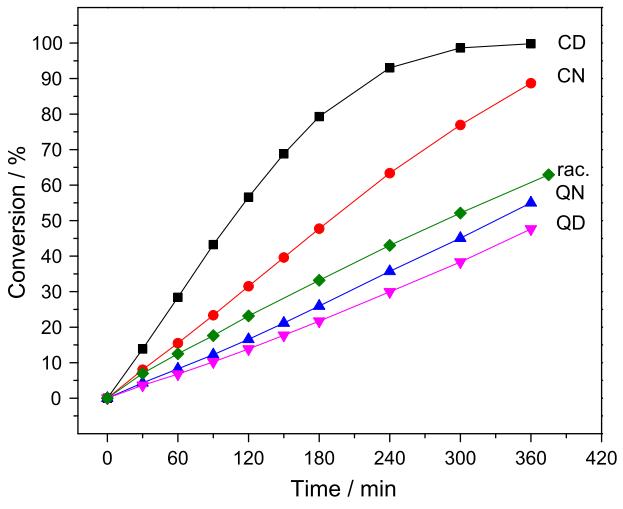

Fig. 1. Effect of different modifiers on the conversion rate of **1** as compared with the racemic hydrogenation (diamonds); CD (squares), CN (circles), QN (up triangles) and QD (down triangles). Conditions: 21 mg catalyst, 3.4 μmol CD, 3.7 mmol **1**, 5 ml toluene, 20 °C, and 3 bar.

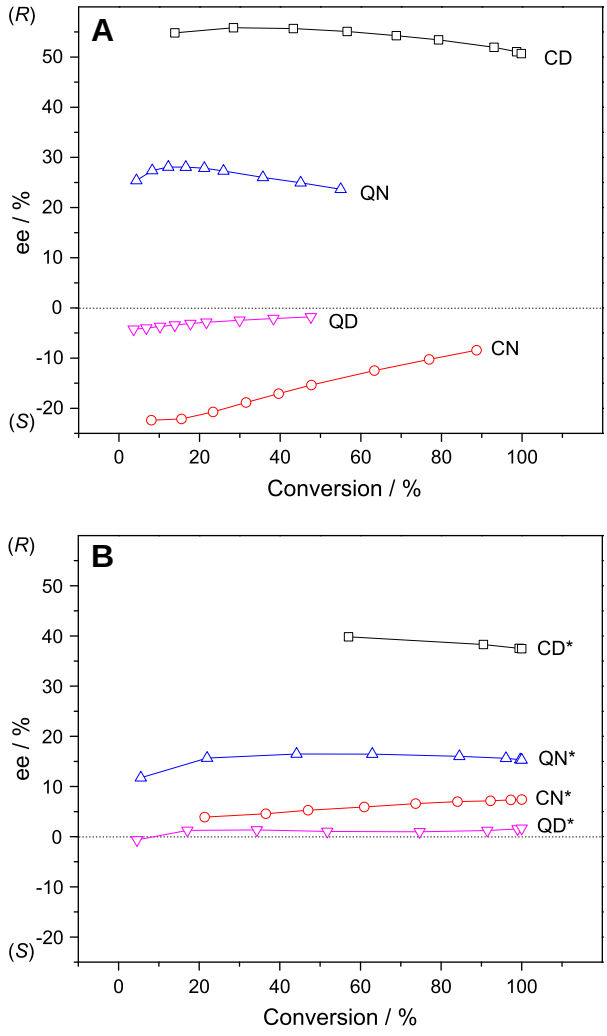

Fig. 2. Effect of initial concentration of **1** on the enantioselectivity. A: 3.7 mmol of **1**; B: 0.93 mmol of **1** (∗ after the abbreviations). Conditions: 21 mg catalyst, 3.4 μmol CD, 5 ml toluene, 20 °C, and 3 bar, reaction time: 6 h.

in Fig. 2B demonstrate that inversion of the major enantiomer of **2** may simply result from a change in the substrate concentration; addition of a strong acid is not a requirement. It is very unlikely that a shift in the substrate concentration would lead to a different reaction mechanism, i.e. a different type of substrate–modifier interaction (N → C=O or N—H—O=C type interaction [25]). This "unexpected inversion" upon changing the substrate concentration may be related to the presence of dimers, trimers, and tetramers of **1** on the Pt surface (at high substrate concentration), as observed recently using scanning tunneling microscopy under UHV conditions [50] and confirmed by NMR in solution, in the absence of Pt and modifier [25]. These observations fit to our concept that the origin of the unusual behavior of the Pt–cinchona system in the hydrogenation of α,α,α-trifluoromethyl ketones is the extensive H-bonding interaction among the reaction partners, including also the product as shown in the next chapter.

*3.2. The role of substrate–modifier–product interactions during hydrogenation of **1***

A specific feature of the hydrogenation of **1** is the enhancement of enantioselectivity at low conversion. In this initial transient period, the ee doubled in 1,2-dichlorobenzene [4]. The phenomenon strongly depends on the reaction conditions and solvent, and variation of the ee with conversion may also be minor [9]. We

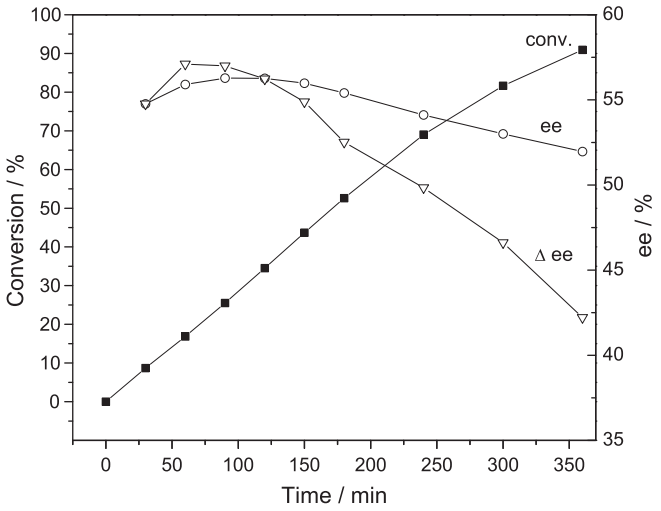

Fig. 3. Conversion (squares), ee (spheres) and differential ee (down triangles) in the hydrogenation of **1**. Conditions 21 mg catalyst, 3.4 μmol CD, 5.5 mmol **1**, 5 ml toluene, 20 °C, and 3 bar.

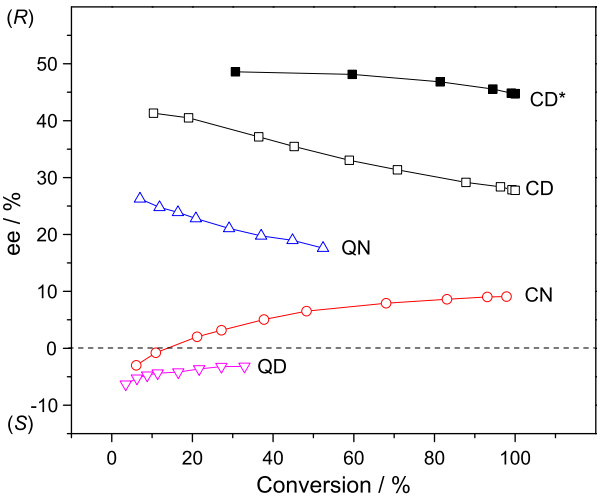

Fig. 4. Hydrogenation of equimolar mixtures of **1** and *rac*-**2** using CD (squares), CN (circles), QN (up triangles) or QD (down triangles). Reference line: CD* (filled squares, no *rac*-**2**). Conditions 21 mg catalyst, 3.4 μmol CD, 1.85 mmol **1** and 1.85 mmol *rac*-**2**, 5 ml toluene, 20 °C, and 3 bar.

found relatively small changes in toluene with CD and QN, but the initial enhancement and the following drop in ee was always clearly distinguishable. A typical example with CD is shown in Fig. 3. The incremental ee indicates that the actual enantioselectivity reached a maximum below 20% conversion and dropped by about 15% till the end of the reaction. Note that in the presence of CN and QD, there was no detectable initial change of direction in the ee–conversion curve, as shown in Fig. 2.

A feasible explanation for the drop in ee with conversion is the interaction of the product α,α,α-trifluoromethyl alcohol with the alkaloid modifier. Due to the presence of the CF_3 group in α-position, the acidity of the OH function increases by several orders of magnitude [52,53]. The polarity and H-bond donor ability (α) of fluorinated alcohols are much higher, while the H-bond acceptor ability (β) is remarkably lower than those of the corresponding non-fluorinated alcohols.

In order to verify our hypothesis, the enantioselective hydrogenation of **1** was carried out in the presence of *rac*-**2** with all four alkaloids (Fig. 4). The initial racemic alcohol concentration was subtracted before calculating the ee. In all these reactions, the ee decreased from the beginning of the reaction. A comparison for CD with and without *rac*-**2** under otherwise identical conditions is also shown to illustrate the shift in the ee–conversion lines. The most interesting observation is that using CN as modifier inversion of the ee was observed with increasing conversion. This example suggests that the effect of increasing amount of product is not simply a decrease of ee but rather a shift to a different mechanism that provides the opposite enantiomer in excess.

3.3. In situ diastereoselective hydrogenation of CD

A deeper insight into the nature of substrate–modifier–product interactions was obtained by studying the chemo- and diastereoselective hydrogenation of the quinoline ring of CD (Scheme 2). This transformation can be investigated under real reaction conditions, in the presence of **1** and **2**, and the product distribution provides direct information on the adsorption mode of CD on the Pt surface [34,35,54], which is not available by any other method.

The first step of the transformation is the fast hydrogenation of the vinyl group of CD (Scheme 2), which is not investigated here. The major characteristics of the hydrogenation of CDH_2 in the absence of substrate or product are presented in Table 1. The dominant product is the (*S*)-CDH_6-A and the de is independent of the conversion. The chemoselectivity, i.e. the ratio of CDH_6-A to CDH_6-B (A/B) is very high, which indicates that saturation of the homoaromatic ring of CD is a minor reaction.

In the presence of **1**, the chemoselectivity dropped significantly (Table 1). The initial rate did not increase but slightly decreased, in contrast to the effect of α-ketoesters [35]. The most important change is the inversion of the major diastereomer of CDH_6-A from (*S*) to (*R*). A similar inversion was observed earlier by changing the solvent from toluene to acetic acid in the absence of any ketone substrate [34], or by addition of an α-ketoester [35]. In addition, the de and also the reaction rate (TOF) increased with increasing conversion of CDH_2. The conversion-dependent changes indicate the strong influence of **2**. An important point here is that the initial de (de_{init}) is very small, although already this value is measured in the presence of a small amount of **2**, since a few percent conversion is necessary to obtain reliable values by GC analysis. It indicates that the de should be around zero and there is no preferred adsorption mode of CD, when the amount of **2** is close to zero. The mechanistic consequences of this observation will be discussed later.

The critical role of the product on the adsorption and hydrogenation of CD is confirmed by the experiment carried out in the presence of equimolar amount of *rac*-**2**. The final de and the chemoselectivity are the same as what was achieved in the presence of **1**, and the rate is also enhanced. The experiments in the presence of (*S*)-**2** or (*R*)-**2** independently revealed that *rac*-**2**, (*S*)-**2** and the reaction mixture formed in the hydrogenation of **1** have similar effects on the rate of the hydrogenation of the quinoline ring and the final des are also very similar. The influence of (*R*)-**2** is different: both the rate and the de of CDH_2 hydrogenation are remarkably higher. It indicates that (*S*)-**2** interacts stronger with the alkaloid and controls its hydrogenation even at a considerable excess of the opposite enantiomer during hydrogenation of **1** (>50% ee to (*R*)-**2**).

Some important details of the analysis of the hydrogenation of CD during the enantioselective hydrogenation of **1** are presented in Figs. 5–7. In the experiment presented in Table 1, the hydrogenation of **1** shows the same behavior (Fig. 5A) as in previous experiments. After an initial increase, the ee decreased continuously with conversion. The differential ee dropped from 60% to less than 40% with conversion. The concomitant hydrogenation of the alkaloid is shown in Fig. 5B, where the rate acceleration with time

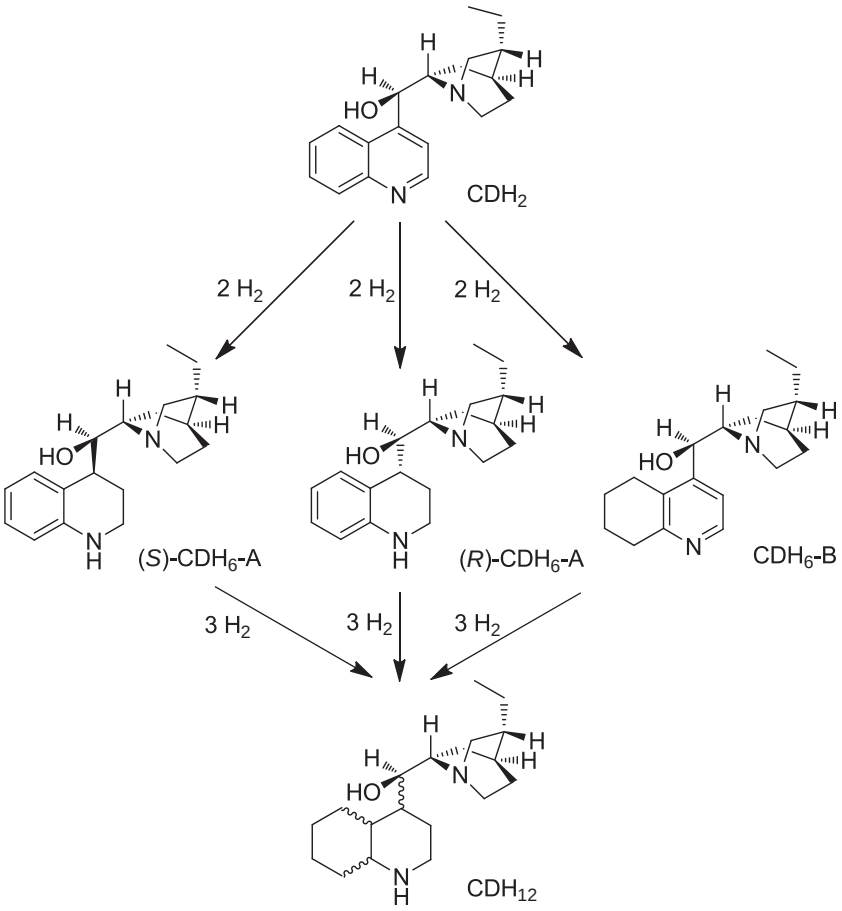

Scheme 2. Chemo- and diastereoselective hydrogenation of 10,11-dihydrocinchonidine (CDH_2).

Table 1
Rates and selectivities in the hydrogenation of CDH_2.[a]

Reaction components	TOF_{init} (h^{-1})	TOF (h^{-1})	de_{init} (%)	de (%)	A/B
CD	1.0	1.0	10 (*S*)	10 (*S*)	31
CD + **1**	0.8	1.2	7 (*R*)	45 (*R*)	12
CD + rac. **2**	2.1	1.6	37 (*R*)	45 (*R*)	12
CD + (*S*)-**2**	1.5	1.3	38 (*R*)	42 (*R*)	10
CD + (*R*)-**2**	6.2	5.9	65 (*R*)	72 (*R*)	22
CD + **1** + TFA	1.5	1.4	69 (*R*)	78 (*R*)	34

[a] Conditions: 42 mg catalyst, 6.8–13.6 μmol CD, 3.7 mmol of **1**, (*R*)-**2**, (*S*)-**2**, or rac. **2**, 10 ml toluene, 25 °C, and 3 bar. CD: TFA = 1:3. TOF_{init} was determined at conversions below 10%, TOF in the conversion range 40–80%, de_{init} and de were calculated similarly.

(conversion) is clearly observable. The large enhancement of the de is also well observable and the differential de indicates stabilization at around 50% conversion of **1**. All these changes in the rate and diastereoselectivity mirror the effect of increasing product concentration.

The negative effect of *rac*-**2** on the enantioselectivity is shown in Fig. 6. The hydrogenation of CD was started in the presence of *rac*-**2** and after 30 min four eq. of **1** was added. The first measured ee value was 49% (Fig. 6A), almost 10% less than what was achieved without the addition of **2** (Fig. 5A). In addition, the ee decreased in the whole conversion range without any initial increase as seen in Fig. 5A. Hydrogenation of CD is affected by the addition of racemic **2**, too (Fig. 6B). In particular, the significant increase especially of the rate and the de to (*R*)-CDH_6-A with conversion was not observed here; the de varied in a relatively narrow range of 40–45% in the whole conversion range. This difference to Fig. 5B proves that the increase in rate and de are due to the interaction of CD with the increasing amount of **2** formed by hydrogenation of **1**.

Finally, the nature of CD–**2** interaction was investigated by the addition of 3 eq. of TFA related to CD (Fig. 7). After an initial increase, the ee in the hydrogenation of **1** remained almost constant; only the differential ee indicates some small decrease above 85% conversion. Also the rate and chemo- and diastereoselectivities in the hydrogenation of the alkaloid are almost constant in the whole concentration range (Table 1). Obviously, addition of only 3 eq. of the strong acid TFA prevents the negative effect of **2** formed in large excess (**2**/CD = up to 1088 molar ratio). In addition, the ee at full conversion improved from 52% to 80% by the TFA additive. These changes indicate that the interaction of CD and **2** involves base–weak acid type interactions, respectively, which are hindered by the interaction with the strong acid TFA.

3.4. NMR investigations

In order to gain more insight into the modifier–product interaction during hydrogenation of **1** on Pt, the catalytic study was completed with NMR experiments. In these experiments, $CDCl_3$ was used as a solvent due to the low solubility of CD in toluene. The negligible effect of solvent was proved in separate experiments using the more soluble QN. A comparison of the ^1H NMR spectra of QN measured in deuterated toluene and $CDCl_3$ revealed no significant differences, implying that the conformations of QN in both solvents are comparable (Supporting information).

The interaction of CD and QN with **1** and **2** was investigated by pulsed gradient spin-echo (PGSE) NMR diffusion experiments. Since the catalytic experiments revealed that the observed

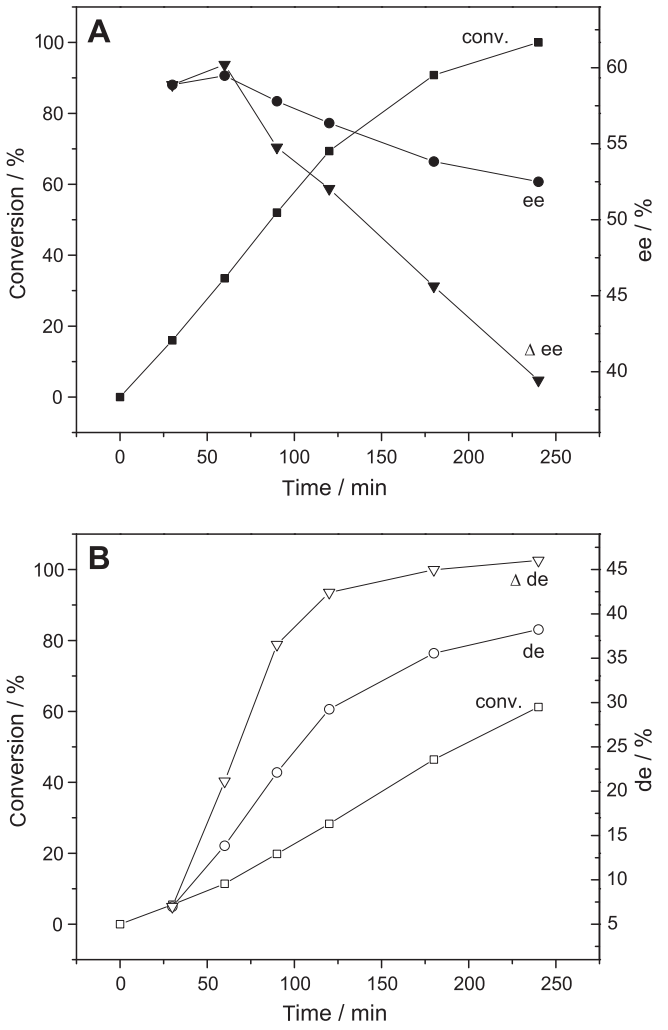

Fig. 5. Conversion (squares), ee (spheres) and differential ee (triangles) in the hydrogenation of **1** in the presence of CD (A). The conversion (squares), de (circles) and differential de (triangles) of the hydrogenation of CDH_2 is shown in part B. Conditions: 42 mg catalyst, 6.8 μmol CD, 7.4 mmol **1**, 10 ml toluene, 25 °C, and 3 bar.

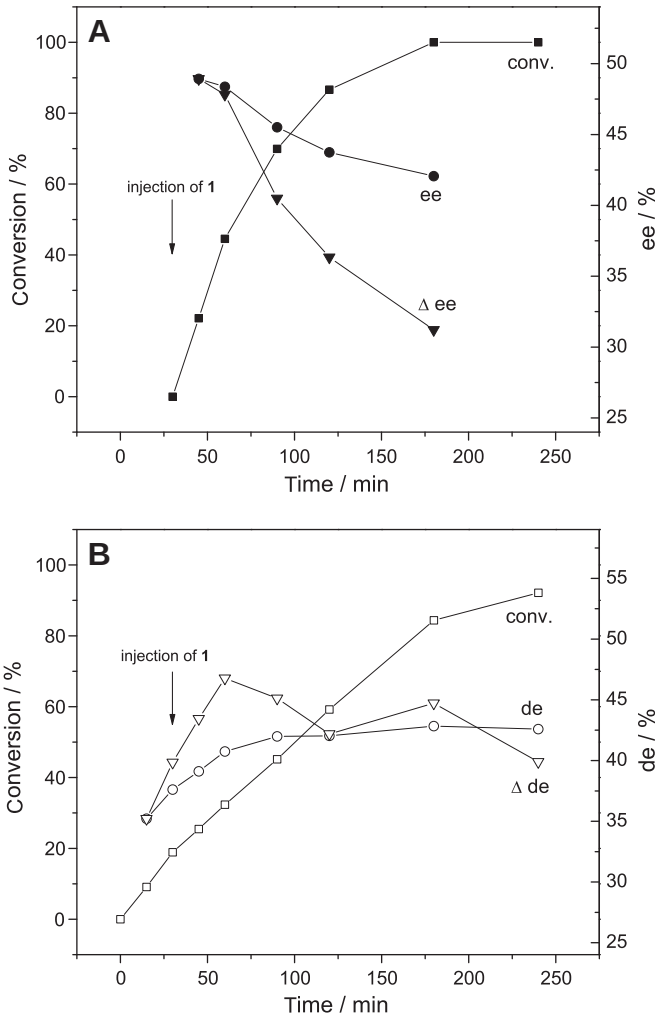

Fig. 6. Conversion (squares), ee (spheres) and differential ee (triangles) in the hydrogenation of **1** injected after 30 min to hydrogenation of CD started with 0.25 eq. of racemic **2** (A). The conversion (squares), de (circles), and differential de (triangles) in the hydrogenation of CDH_2 is shown in part B. Conditions: 42 mg catalyst, 6.8 μmol CD, 7.4 mmol **1**, 1.85 mmol *rac*-**2**, 10 ml toluene, 25 °C, and 3 bar.

catalytic behavior is dominated by the presence of (*S*)-**2** (Table 1), we considered this enantiomer for the diffusion study. Determination of the diffusion coefficients *D* allow to calculate the hydrodynamic radii r_H via the Stokes–Einstein equation (Eq. (3)) [39],

$$D = \frac{kT}{c\pi\eta r_H} \tag{3}$$

where *k* is the Boltzmann constant, *T* the absolute temperature, *c* the friction constant, η the solution viscosity, and r_H the hydrodynamic radius.

The comparison of the calculated hydrodynamic radii of (*S*)-**2** from the experiments carried out with and without CD revealed a significant bigger radius in the former case (Table 2). A similar effect was observed when QN was used as the modifier. In contrast, no effect of the cinchona modifier on the diffusion behavior of **1** was detectable.

The increase of the hydrodynamic radius demonstrates the interactions between the modifier and (*S*)-**2**. The fact that only small changes of *D* and r_H were observed can be rationalized by assuming a fast equilibrium between solvated and complexed (*S*)-**2**, whereby the equilibrium lies on the side of the solvated (*S*)-**2**. The absence of significant changes of *D* and r_H in the experiments with **1** indicates that the interaction between **1** and the

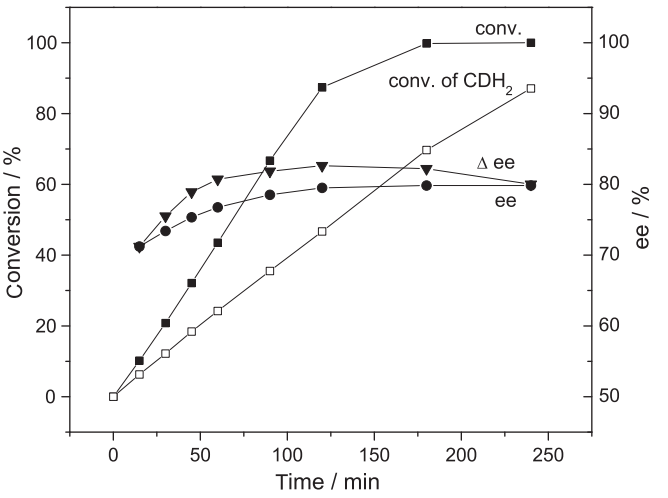

Fig. 7. Conversion (squares), ee (spheres), and differential ee (triangles) in the hydrogenation of **1** (filled symbols) in the presence of 3 eq. of TFA related to CD. The concomitant conversion of CDH_2 is shown with empty squares. Conditions: 42 mg catalyst, 6.8 μmol CD, 7.4 mmol **1**, 10 ml toluene, 0 °C, and 10 bar.

Table 2
Diffusion coefficients D (10–10 $m^2 s^{-1}$) and hydrodynamic radii r_H derived from ^1H and ^{19}F diffusion experiments for (*S*)-**2**, **1** + modifier in $CDCl_3$ at 298 K[a] (mean values).

	2	
	D	r_H (Å)
(*S*)-**2**	17.05	2.4
(*S*)-**2** + CD	16.37	2.5
(*S*)-**2** + QN	16.27	2.5
	1	
1	17.83	2.3
1 + CD	17.88	2.3

[a] η ($CHCl_3$) = 0.53 × 10^{-3} kg s^{-1} m^{-1}.

modifier is much weaker than that between **2** and the modifier, and the complexation equilibrium remains essentially completely on the side of the non-interacting **1**.

These results were corroborated by 1D ^{19}F NMR measurements, where the addition of modifier to the solution of **1** did not induce any shift of the signal of the CF_3 group. In the case of **2**, however, a significant shift by 0.17 ppm of the signal was observed (QN + (*S*)-**2**, Supporting information, Figs. 5-1 and 5-2). The phenomenon has already been reported by Abid et al., who used cinchona alkaloids to determine the ee of α-trifluoromethylated-hydroxyl compounds by ^{19}F NMR spectroscopy [55].

To elucidate the interactions between **2** and the modifier, 1D ^1H NMR spectra of 10 mM solutions of QN or CD + (*R*)-**2** or (*S*)-**2** (molar ratio 1:1) were recorded in $CDCl_3$. The graphical comparison to the corresponding spectra of pure QN or CD in $CDCl_3$ is shown in Figs. 8 and 9, respectively. Major shift differences in both modifiers were observed for the protons H8–H11 (Scheme 3). The shielding of H9 and H11 and deshielding of H10 indicates a counterclockwise rotation of the quinuclidine moiety around the C8—C9 bond (Scheme 1), which places H9 and H11 over the aromatic ring of quinoline and H10 next to it [56]. The possible reasons for the deshielding of H8 are manifold. It may be caused partly by the rotation of the quinuclidine fragment or by a hydrogen bond between the quinuclidine N and **2**. In both cases, the shielding effect of the N lone pair is reduced probably leading to the observed deshielding of H8.

The presence of either (*R*)-**2** or (*S*)-**2** lead as well to an increase of the vicinal $^3J_{H_8H_9}$ coupling constant, which is sensitive to the rotation of the quinuclidine moiety around the C8—C9 bond (Table 3). In comparison, the interaction of (*S*)-**2** seems to introduce a larger rotation around the C8—C9 bond than (*R*)-**2** as evidenced by its bigger $^3J_{H_8H_9}$. Consequently, the corresponding ^1H, ^1H NOESY experiments on samples of both modifiers with (*R*)-**2** and (*S*)-**2** showed NOE contacts between H1 and H8, H9, H10, H14 and H16, and between H5 and H8, H9 and H16, respectively (Supporting information Figs. 6-1 to 6-4), indicating an Open(3) conformation of the modifier [57]. In addition, the strong NOE contact between H1 and H10 supports close proximity of the latter to the quinoline ring.

In order to locate possible interactions between the modifier and **2**, ^1H, ^{19}F HOESY experiments were carried out. Besides the intramolecular interactions of the CF_3 group with the aromatic ortho protons of **2** and its aliphatic proton on the C atom bearing the OH group, a strong intermolecular NOE contact with the protons of the methoxy group on C6′ in QN was observed (Fig. 10) for both enantiomers of **2**. In the case of CD and **2**, there is no clear evidence of an analogous interaction of the CF_3 group with H6 due to the presence of potentially overlapping NOE cross peaks to the aromatic ortho protons of **2**. However, a comparison of the chemical shift differences (in the absence and presence of **2**) of the protons in CD and the protons in QN suggests that **2** interacts with both modifiers in a similar way (Figs. 8 and 9). The interaction of the CF_3 group with the methoxy protons in QN and the similarities in the interaction of **2** with both modifiers may result from hydrogen bonding between the OH group of **2** and the quinuclidine N atom.

In summary, based on our NMR data, we suggest a significant interaction of the hydrogenation product **2** with the modifier. In the complexation product, the HO function of **2** seems to be residing close to the quinuclidine N atom, presumably due to hydrogen bonding of the OH group with the latter. This H-bonding interaction between the alcohol and the modifier induces some conforma-

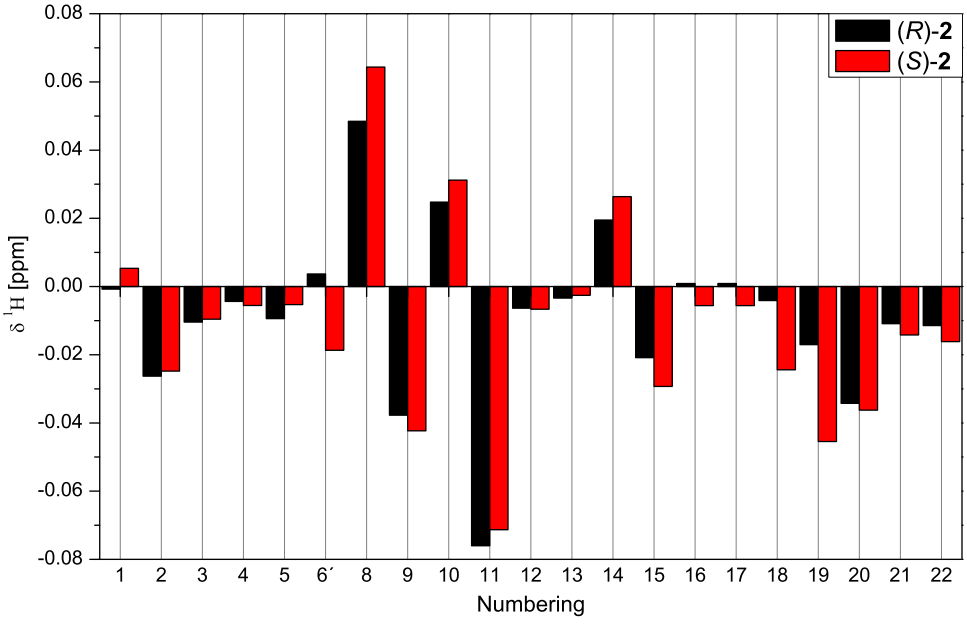

Fig. 8. Chemical shift differences in ^1H NMR spectra of QN in the presence of (*R*)-**2** and (*S*)-**2** in $CDCl_3$ (molar ratio 1:1). Numbering of protons is shown in Scheme 3.

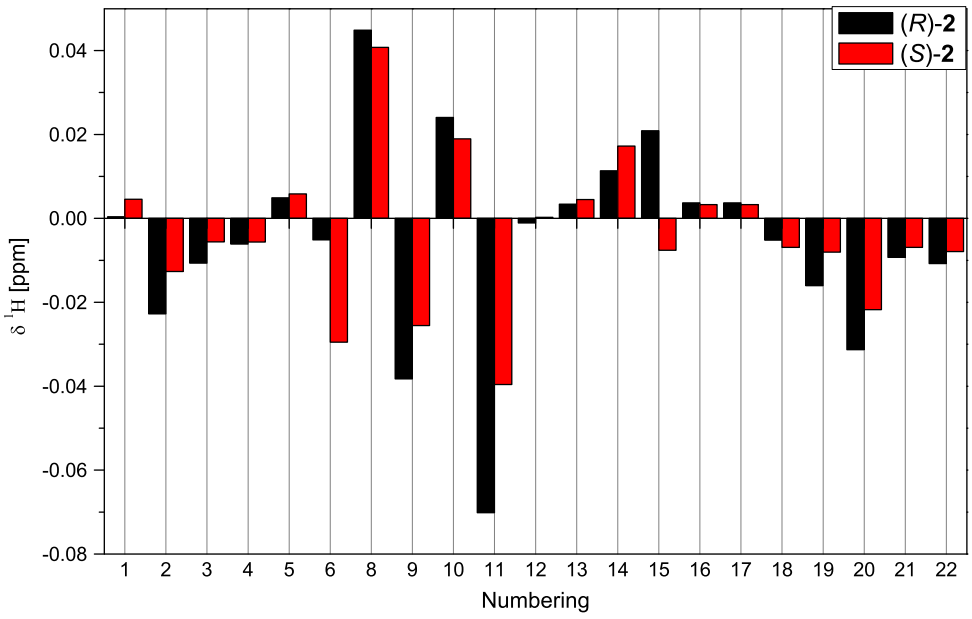

Fig. 9. Chemical shift differences in ^{1}H NMR spectra of CD in the presence of (*R*)-**2** and (*S*)-**2** in $CDCl_3$ (molar ratio 1:1). Numbering of protons is shown in Scheme 3.

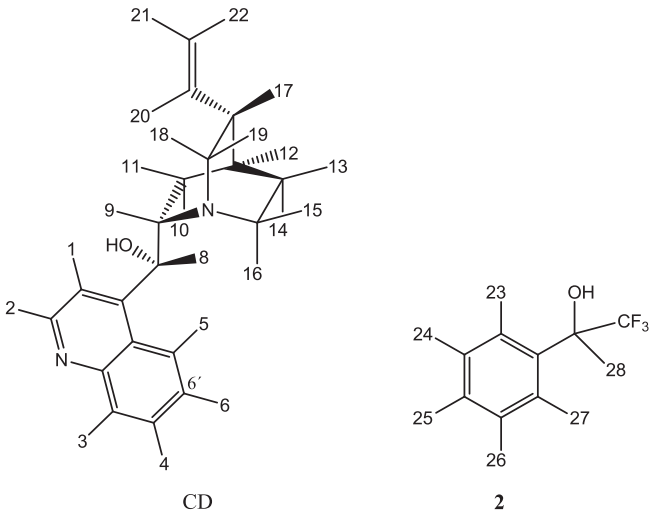

Scheme 3. CD and **2** proton numbering.

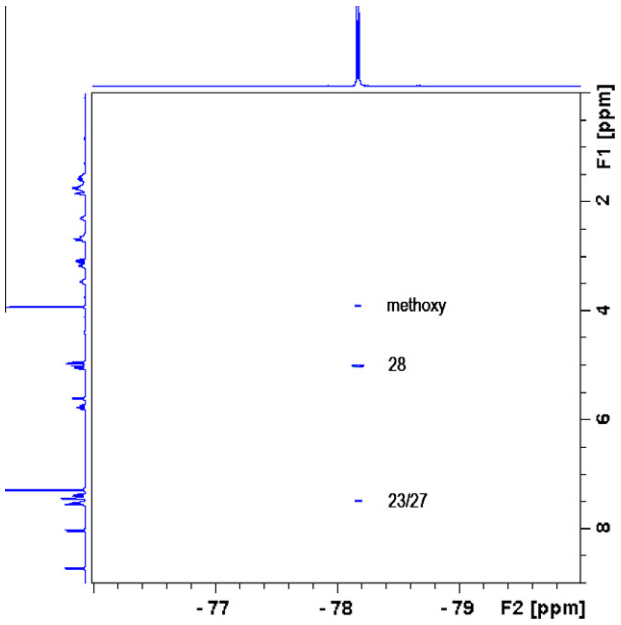

Fig. 10. ^{19}F, ^{1}H HOESY spectrum of (*S*)-**2** with QN in $CDCl_3$; molar ratio 1:1.

Table 3
Vicinal $^3J_{H_8H_9}$ coupling constants for quinine (QN) and cinchonidine (CD) in the presence of (*R*)-**2** and (*S*)-**2** in $CDCl_3$.[a]

	QN	CD
Modifier	2.4	3.0
Modifier + (*R*)-**2**	2.7	3.9
Modifier + (*S*)-**2**	3.6	4.1

[a] The accuracy of measured coupling constants is 0.1 Hz.

tional changes in the modifier, the most prominent being the rotation around the C8—C9 bond. This interaction is expected to be relatively strong due to the acidity and increased H-bond donor ability of the α,α,α-trifluoromethyl alcohol **2** [52,53]. There is an indication to an additional interaction between an H atom of the C6′-methoxy group of QN and the CF_3 group of **2**, but an analogous interaction with the C6' H atom of CD could not be evidenced.

3.5. Mechanistic considerations

Three fundamentally different mechanistic concepts have been brought up to interpret the stereochemical outcome of the hydrogenation of α,α,α-trifluoromethyl ketones on cinchona-modified Pt. The most recent model proposed by Bartók and coworkers [25–27] and its contradiction to some fundamental experimental observations have already been discussed in the previous chapters.

The essence of our model developed for the hydrogenation of activated ketones is a single attractive interaction, an N—H—O type bond, between the quinuclidine N of the modifier and the keto carbonyl group of the substrate [17]. The model is based on an in situ spectroscopic observation [32]. The adsorption of the ketone on the Pt surface is assumed to be controlled by electronic interactions between the alkaloid and the activating (electron

withdrawing) function of the ketone. A direct involvement of the quinoline ring of the modifier was rejected based on missing steric effects in the hydrogenation of bulky α-ketoesters [58]. The unique behavior of the hydrogenation of α-fluorinated ketones is attributed to additional H-bonding interactions; the clearest example among them is the sometimes striking changes in enantioselectivity induced by addition of TFA [6,24].

McBreen and coworkers described various prochiral complexes responsible for enantioselection [50,59–61]. A common point in these models, based on STM studies under ex situ conditions, is a double substrate–modifier interaction involving not only the quinuclidine N atom but also one or two H atoms of the quinoline ring. This concept is, however, in contrast to the in situ investigation of the hydrogenation of CD. The results in Table 1 show that during hydrogenation in toluene in the absence of substrate or other additive, the adsorption mode of CD on Pt is slightly dominated by the pro(*S*) geometry, leading to the formation of (*S*)-CDH_6-A upon hydrogenation. This adsorption mode is illustrated in Scheme 4, left. Notice, however, the very small excess: at 10% de the product mixture corresponds to a 55:45 ratio. Addition of the substrate (**1**) barely changes this ratio. The minor initial de of 7% to (*R*)-CDH_6-A is probably due to the presence of small amounts of the stronger interacting (*S*)-**2**, as discussed in the previous chapter. This result is in good agreement with those of ex situ NMR diffusion experiments indicating weak interaction of the alkaloid with **1** and stronger interaction with **2**. By the end of the reaction or by adding only (*S*)-**2**, the de increases to 42–45% (*R*)-CDH_6-A, which corresponds to a dominant pro(*R*) adsorption mode of CD (Scheme 4, right). The major difference between the two adsorption modes is the inverted position of the quinoline ring. McBreen's model implicitly assumes the pro(*R*) adsorption mode of CD, which would enable a second interaction with the substrate. In contrast, at the early stage of the hydrogenation of **1** the data in Table 1 do not show a significant preference to this adsorption mode. Obviously, the diastereoselective hydrogenation of CD disproves the importance of a second interaction between **1** and an aromatic H of CD.

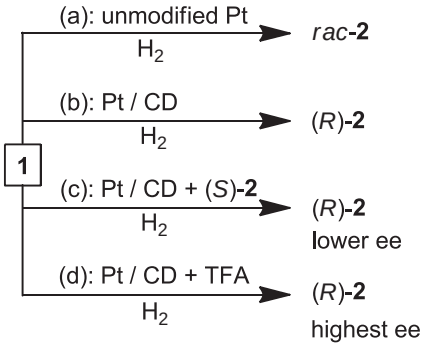

Scheme 5. Multiple cycle mechanism in the hydrogenation of 2,2,2-trifluoroacetophenone (**1**) to 1-phenyl-2,2,2-trifluoroethanol (**2**) on the Pt–CD system.

3.6. Multiple cycle mechanism in the enantioselective hydrogenation of *1*

We propose a multiple cycle mechanism for the interpretation of the unique behavior of α,α,α-trifluoromethyl ketones, compared with those of other activated ketones. The starting point is the two-cycle mechanism commonly accepted for chirally modified metals [47,62]. The basic assumption is that not all surface metal sites are chirally modified and the unmodified sites provide racemic product (route *a* in Scheme 5). The contribution of this route is important at low modifier concentration that leads to incomplete surface modification and lower (overall) ee.

On the chirally modified surface, the substrate–modifier interaction results in the preferential formation of one enantiomer, in the present case (*R*)-**2** (route *b* in Scheme 5). This route is impor-

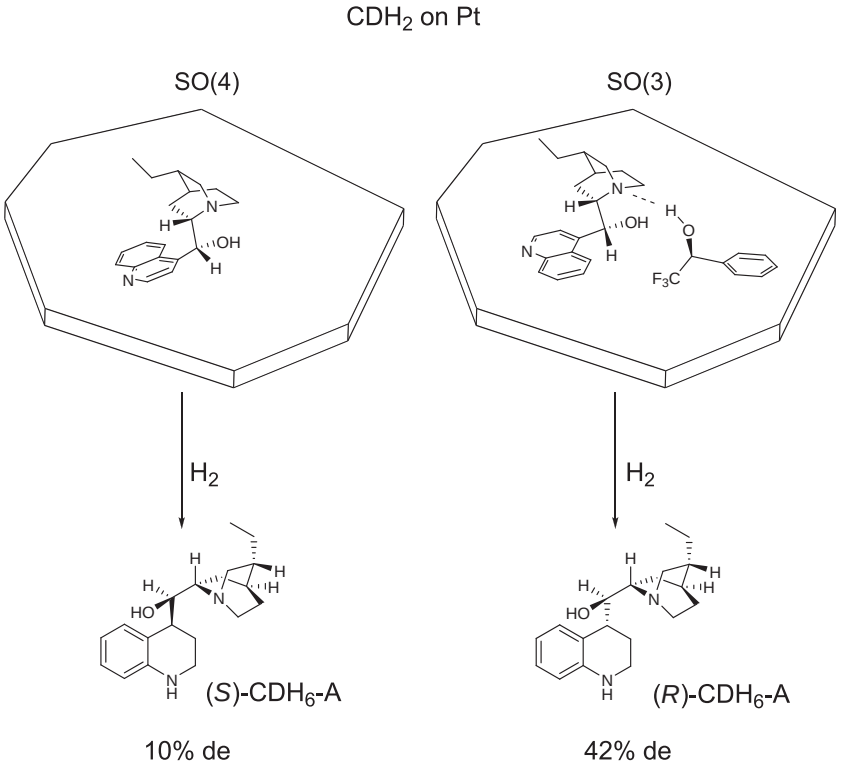

Scheme 4. Hydrogenation of 10,11-dihydrocinchonidine (CDH_2) on the Pt surface alone (left) and in the presence of (*S*)-**2** (right) in toluene.

tant only at the early stage of the reaction, until the concentration of the α-fluorinated alcohol is very low.

To interpret our observations in the enantioselective hydrogenation of **1** on cinchona-modified Pt, we have to introduce two more cycles. The enantioselective hydrogenation of **1** and the in situ diastereoselective hydrogenation of CD in the presence of **1** and **2** revealed a strong interaction between the alkaloid and (*S*)-**2**. Importantly, this interaction is remarkably stronger than the alkaloid–**1** interaction (route *b*). Parallel to the formation of the minor enantiomer (*S*)-**2**, the alkaloid is transformed to an alkaloid–(*S*)-**2** complex (Scheme 4, right) and this complex becomes the actual modifier (route *c* in Scheme 5). This switch in the mechanism is reflected by lower ees to (*R*)-**2** with increasing conversion, and in case of CN even the major enantiomer is inverted (Fig. 4). It is reasonable to assume that this deviation from the general behavior of activated ketones is due to the acidic and strong H-bond donor character of the α-trifluoromethyl alcohol product [52,53]. The acidic OH function should interact strongly with the basic quinuclidine N of the alkaloid, and this assumption is supported by the (ex situ) NMR measurements.

A less clear point is the second, weaker interaction between (*S*)-**2** and the alkaloid, which is not indicated in Scheme 4. The NMR study confirmed the interaction involving the F atoms of (*S*)-**2** and the H atoms of the 6′-methoxy group of QN, but a similar interaction involving the H atoms at C6' could not be clarified unambiguously. Due to steric and electronic effects, the strength of these interactions should be remarkably different for CD and QN and may be related to the different efficiency of these modifiers (see Figs. 1 and 2 and Refs. [25–27]). An important point is that the remarkably stronger interaction of the (*S*)-**2** isomer with CD, compared with the (*R*)-**2**–CD interaction, proves unambiguously that the second interaction is important and sterically demanding. In case of a single interaction of the acidic OH function of **2** with the quinuclidine N atom, no difference between the two enantiomers would exist. In this respect, a clear limitation of the NMR study is that we could not use the same solvent, which was applied in catalytic studies.

Addition of the strong acid TFA (p*K*a = 0.2) is commonly used to improve the ee in the hydrogenation of α-fluorinated ketones [6,24]. TFA replaces the weak acid (*S*)-**2** (p*K*a = 11.9 [63]), and the base–strong acid type alkaloid–TFA complex provides higher ee to (*R*)-**2** (Fig. 7). Due to the large difference in acidity, this cycle (route *d* in Scheme 5) is dominant already in the presence of only three equivalents of TFA related to CD, despite the large excess of (*S*)-**2** in the reaction mixture. Comparing all cases depicted in Scheme 5, the pro(*R*) adsorption mode of CDH_2 is the most dominant in case of the TFA–CD complex, as indicated by the highest de of 78% to (*R*)-CDH_6-A (Table 1). The structures of TFA–CD complexes have been described elsewhere [64]. Note that similar structures have to be considered in case of AcOH, but those complexes are less stable due to the weaker acidity, compared with TFA [24].

We assume that the aforesaid considerations are valid also to other α,α,α-trifluoromethyl ketones, since the origin of their unique behavior is the acidic (H-bond donor) character of the product alcohol and the H-bond acceptor ability of the CF_3 group. Note that in the hydrogenation of other activated ketones, including the mostly studied α-ketoesters, the product is not acidic and thus its involvement in the mechanism is not expected. This possibility was excluded already in the nineties in case of ethyl pyruvate. Margitfalvi and Hegedüs [65] found that "the form of the optical yield vs. conversion dependencies was not altered by addition of (*R*)-ethyl lactate", in contrast to our present observations. Furthermore, the biggest effect on the ee caused by the addition of ethyl lactate was only 1.1%, barely exceeding the probable experimental error. Clearly, ethyl lactate had no significant influence on the enantioselection.

4. Conclusions

There have been several important experimental observations in the enantioselective hydrogenation of α,α,α-trifluoromethyl ketones on cinchona-modified Pt that could not be rationalized by the existing mechanistic models. In the present study, we focus on the special role of the product, which is yet unprecedented in the hydrogenation of other activated ketones. We propose a new mechanistic concept for the enantioselective hydrogenation of 2,2,2-trifluoroacetophenone (**1**). This multiple cycle mechanism includes four competing cycles, one racemic and three enantioselective routes to 1-phenyl-2,2,2-trifluoroethanol (**2**). The primary origin of enantioselection is (i) an N—H—O bond between the quinuclidine N of the alkaloid and the carbonyl O of the substrate and (ii) the chiral environment provided by the alkaloid. The unique behavior of α-fluorinated ketones is attributed to additional H-bonding interactions of the quinuclidine N with the acidic product or the acid additive. The importance of these cycles in enantioselection is determined by the relative strength of interactions: CD–**1** < CD–(*S*)-**2** < CD–TFA. Since the basis of these additional cycles is the acidic character of the fluorinated alcohol product, the mechanistic model is expected to be valid also for other representatives of α-fluoromethyl ketones.

Acknowledgment

Financial support of this work by the Swiss National Science Foundation is kindly acknowledged.

Appendix A. Supplementary material

Supplementary data associated with this article can be found, in the online version, at doi:10.1016/j.jcat.2011.03.009.

References

[1] Y. Orito, S. Imai, S. Niwa, N.G. Hung, J. Synth. Org. Chem. 37 (1979) 173.
[2] H.U. Blaser, Tetrahedron: Asymmetry 2 (1991) 843–866.
[3] G. Webb, P.B. Wells, Catal. Today 12 (1992) 319–337.
[4] T. Mallat, M. Bodmer, A. Baiker, Catal. Lett. 44 (1997) 95–99.
[5] M. von Arx, T. Mallat, A. Baiker, Tetrahedron: Asymmetry 12 (2001) 3089–3094.
[6] M. von Arx, T. Mallat, A. Baiker, Catal. Lett. 78 (2002) 267–271.
[7] K. Balàzsik, B. Török, K. Felföldi, M. Bartók, Ultrason. Sonochem. 5 (1999) 149–155.
[8] R. Hess, S. Diezi, T. Mallat, A. Baiker, Tetrahedron: Asymmetry 15 (2004) 251–257.
[9] T. Varga, K. Felföldi, P. Forgó, M. Bartók, J. Mol. Catal. A: Chem. 216 (2004) 181–187.
[10] A. Vargas, F. Hoxha, N. Bonalumi, T. Mallat, A. Baiker, J. Catal. 240 (2006) 203–212.
[11] H.U. Blaser, H.P. Jalett, D.M. Monti, A. Baiker, J.T. Wehrli, Stud. Surf. Sci. Catal. 67 (1991) 147–155.
[12] E. Talas, J.L. Margitfalvi, Chirality 22 (2010) 3–15.
[13] M. Studer, H.U. Blaser, C. Exner, Adv. Synth. Catal. 345 (2003) 45–65.
[14] T. Bürgi, A. Baiker, Acc. Chem. Res. 37 (2004) 909–917.
[15] D.Y. Murzin, P. Maki-Arvela, E. Toukoniitty, T. Salmi, Catal. Rev. Sci. Eng. 47 (2005) 175–256.
[16] M. Bartók, Curr. Org. Chem. 10 (2006) 1533–1567.
[17] T. Mallat, E. Orglmeister, A. Baiker, Chem. Rev. 107 (2007) 4863–4890.
[18] F. Zaera, J. Phys. Chem. C 112 (2008) 16196–16203.
[19] M. von Arx, T. Mallat, A. Baiker, in: D.C. Sherrington, A.P. Kybett (Eds.), Supported Catalysts and their Applications, The Royal Soc. Chem., Cambridge, 2001, pp. 247–254.
[20] M. von Arx, T. Mallat, A. Baiker, J. Catal. 193 (2000) 161–164.
[21] K. Felföldi, T. Varga, P. Forgó, M. Bartók, Catal. Lett. 97 (2004) 65–70.
[22] M. von Arx, T. Mallat, A. Baiker, J. Catal. 202 (2001) 169–176.
[23] D. Ferri, T. Bürgi, A. Baiker, J. Chem, Soc. Perkin Trans. 2 (1999) 1305–1311.
[24] M. von Arx, T. Bürgi, T. Mallat, A. Baiker, Chem. Eur. J. 8 (2002) 1430–1437.
[25] K. Szöri, K. Balazsik, S. Cserenyi, G. Szollosi, M. Bartok, Appl. Catal. A: Gen. 362 (2009) 178–184.
[26] G. Szöllösi, S. Cserènyi, M. Bartók, Catal. Lett. 134 (2010) 264–269.
[27] G. Szöllösi, S. Cserényi, I. Bucsi, T. Bartók, F. Fülöp, M. Bartók, Appl. Catal. A: Gen. 382 (2010) 263–271.
[28] M. Bartók, Chem. Rev. 110 (2010) 1663–1705.

[29] W.-R. Huck, T. Bürgi, T. Mallat, A. Baiker, J. Catal. 200 (2001) 171–180.
[30] A. Vargas, T.B. Bürgi, A. Baiker, J. Catal. 222 (2004) 439–449.
[31] A. Vargas, T. Bürgi, A. Baiker, J. Catal. 226 (2004) 69–82.
[32] N. Bonalumi, T. Bürgi, A. Baiker, J. Am. Chem. Soc. 125 (2003) 13342–13343.
[33] I.C. Lee, R.I. Masel, J. Phys. Chem. B 106 (2002) 368–373.
[34] E. Schmidt, W. Kleist, F. Krumeich, T. Mallat, A. Baiker, Chem. Eur. J. 16 (2010) 2181–2192.
[35] E. Schmidt, T. Mallat, A. Baiker, J. Catal. 272 (2010) 140–150.
[36] R.K. Harris, E.D. Becker, S.M.C. De Menezes, R. Goodfellow, P. Granger, Pure Appl. Chem. 73 (2001) 1795–1818.
[37] E.O. Stejskal, J.E. Tanner, J. Chem. Phys. 42 (1965) 288–292.
[38] P.S. Pregosin, Prog. Nucl. Magn. Reson. Spectrosc. 49 (2006) 261–288.
[39] P.S. Pregosin, P.G.A. Kumar, I. Fernandez, Chem. Rev. 105 (2005) 2977–2998.
[40] A. Gierer, K. Wirtz, Z. Naturfors, Sect. A: J. Phys. Sci. 8 (1953) 532–538.
[41] H.C. Chen, S.H. Chen, J. Phys. Chem. 88 (1984) 5118–5121.
[42] S. Macura, R.R. Ernst, Mol. Phys. 41 (1980) 95–117.
[43] S.J. Archer, D.M. Baldisseri, D.A. Torchia, J. Magn. Reson. 97 (1992) 602–606.
[44] P.L. Rinaldi, J. Am. Chem. Soc. 105 (1983) 5167–5168.
[45] Z. Ma, F. Zaera, J. Phys. Chem. B 109 (2005) 406–414.
[46] L. Mink, Z. Ma, R.A. Olsen, J.N. James, D.S. Sholl, L.J. Mueller, F. Zaera, Top. Catal. 48 (2008) 120–127.
[47] M. Garland, H.U. Blaser, J. Am. Chem. Soc. 112 (1990) 7048.
[48] E. Toukonitty, D.Y. Murzin, J. Catal. 241 (2006) 96–102.
[49] M. Studer, S. Burkhardt, H.U. Blaser, Chem. Commun. (1999) 1727–1728.
[50] M.A. Laliberte, S. Lavoie, B. Hammer, G. Mahieu, P.H. McBreen, J. Am. Chem. Soc. 130 (2008) 5386–5387.
[51] H.U. Blaser, M. Studer, Accounts Chem. Res. 40 (2007) 1348–1356.
[52] J.P. Begue, D. Bonnet-Delpon, B. Crousse, Synlett (2004) 18–29.
[53] R.E. Ramirez, C. Garcia-Martinez, F. Mendez, J. Phys. Chem. A 113 (2009) 10753–10758.
[54] E. Schmidt, F. Hoxha, T. Mallat, A. Baiker, J. Catal. 274 (2010) 117–120.
[55] M. Abid, B. Török, Tetrahedron: Asymmetry 16 (2005) 1547–1555.
[56] R.S. Macomber, A Complete Introduction to Modern NMR Spectrsocopy, Wiley, New York, 1998.
[57] T. Bürgi, A. Baiker, J. Am. Chem. Soc. 120 (1998) 12920–12926.
[58] S. Diezi, S. Reimann, N. Bonalumi, T. Mallat, A. Baiker, J. Catal. 239 (2006) 255–262.
[59] S. Lavoie, G. Mahieu, P.H. McBreen, Angew. Chem. Int. Ed. 45 (2006) 7404–7407.
[60] S. Lavoie, M.A. Laliberte, I. Temprano, P.H. McBreen, J. Am. Chem. Soc. 128 (2006) 7588–7593.
[61] V. Demers-Carpentier, M.A. Laliberte, S. Lavoie, G. Mahieu, P.H. McBreen, J. Phys. Chem. C 114 (2010) 7291–7298.
[62] J.T. Wehrli, Thesis, ETH, Zürich, 1989.
[63] R. Stewart, R. van der Linden, Can. J. Chem.: Rev. Can. Chim. 38 (1960) 399–406.
[64] W.-R. Huck, T. Bürgi, T. Mallat, A. Baiker, J. Catal. 205 (2002) 213–216.
[65] J.L. Margitfalvi, M. Hegedüs, J. Mol, Catal. A: Chem. 107 (1996) 281–289.